

Transition spectra for a BCS superconductor with multiple gaps: Model calculations for MgB₂

Sergey V. Barabash and David Stroud

Department of Physics, The Ohio State University, Columbus, Ohio 43210

(Received 19 February 2002; revised manuscript received 12 August 2002; published 4 November 2002)

We analyze the qualitative features in the transition spectra of a model superconductor with multiple energy gaps, using a simple extension of the Mattis-Bardeen expression for probes with case I and case II coherence factors. At temperature $T=0$, the far-infrared absorption edge is, as expected, determined by the smallest gap. However, the large thermal background may mask this edge at finite temperatures and instead the secondary absorption edges found at $\Delta_i + \Delta_j$ may become most prominent. At finite T , if certain interband matrix elements are large, there may also be absorption peaks at the gap difference frequencies $|\Delta_i - \Delta_j|/\hbar$. We discuss the effect of sample quality on the measured spectra and the possible relation of these predictions to the recent infrared absorption measurement on MgB₂.

DOI: 10.1103/PhysRevB.66.172501

PACS number(s): 74.25.Gz, 74.20.-z

Among the unusual features of superconductivity in MgB₂ is the widely discussed possibility that there may exist several distinct energy gaps. The larger gap or gaps are thought to be associated with electrons in the boron p_{xy} bands, frequently referred to as “two-dimensional(2D) bands” because of their very weak dependence on k_z , the component of \mathbf{k} parallel to the c axis. These bands appear to be strongly coupled to a particular (E_{2g}) phonon mode and are believed primarily responsible for the high superconducting T_c (~ 40 K). Interactions between these 2D electrons and those in other bands (specifically, the “3D” bands formed by the B p_z states) lead to superconducting gaps in the spectra of these other electrons. A multiple-gap structure can be described either with a simple BCS framework¹ or by more detailed *ab initio* calculations using the Eliashberg theory.² The result of such theories is that the average 2D gap Δ_{2D} is about 3 times larger than Δ_{3D} .³ These predictions are supported experimentally by heat capacity,^{2,4,5} tunneling,⁶⁻⁹ photoemission,¹⁰ and penetration depth¹¹ measurements.

In this work, we present a simple model calculation of the transition spectra in a superconductor with multiple gaps, using a natural extension of the Mattis-Bardeen (MB) formulas.¹² We find that this model is not only consistent with the observed infrared absorption edge in MgB₂, which occurs at anomalously low frequencies relative to the single-gap BCS prediction, but also predicts that a characteristic additional structure in the absorption may be observed under certain conditions.

In our calculations, we consider only the effects of multiple gaps on coherence phenomena and on the superconducting density of states, and neglect nonlocal electrodynamic effects. Such an approximation is known to become exact in either the dirty limit ($l \ll \xi_0$, where l is the quasiparticle mean-free path and ξ_0 is the coherence length) or the “extreme anomalous” limit ($k\xi_0 \gg 1$, where k is the wave vector of the perturbation). In fact, neither of these limits may actually be applicable to samples of MgB₂ with multiple gaps (in particular, a single gap would normally be expected in the dirty limit.¹³). Nevertheless, previous calculations suggest that the MB formalism gives at least a reasonable qualitative description of experiment in single-gap superconductors, even when used beyond its nominal validity limit. The calculation is also very easy. Thus, it is reasonable to do such

a calculation as a first step in understanding the absorption spectra in MgB₂. Various further corrections should be included in the strong-coupling limit,¹⁵ although they may not change the calculated absorption spectra qualitatively.¹⁶

We adopt a BCS-like multiple-gap model proposed by Liu *et al.*¹ In this model, the self-consistent gap equation is written as

$$\Delta_i = \sum_j U_{ij} \Delta_j \int_{-\omega_D}^{\omega_D} N_j(\xi) \frac{\tanh(\beta E_j(\xi)/2)}{E_j(\xi)} d\xi, \quad (1)$$

where $\beta = 1/k_B T$, with T the temperature, Δ_i one of the n gaps, U_{ij} the corresponding $n \times n$ effective phonon-mediated electron-electron interaction matrix calculated in Ref. 1, $N_i(\xi)$ the normal density of states for the i th band, and $E_i(\xi) = \sqrt{\Delta_i^2 + \xi^2}$, $\xi = \epsilon - \mu$ (where ϵ is the single-particle energy and μ is the Fermi energy). Finally, ω_D is a cutoff energy, which is assumed to be the same for all n bands. The solution of the n equations (1) gives $\Delta_i(T)$. In a single-gap BCS superconductor ω_D is of order the Debye frequency. In MgB₂ the value $\omega_D \approx 7.5$ meV needed to produce $T_c \approx 40$ K is much smaller than the physically relevant logarithmically averaged phonon frequency $\omega_{\text{ln}} = 56.2$ meV (Ref. 1); this discrepancy would probably be removed by the inclusion of strong-coupling corrections omitted from Eq. (1). In any case, the BCS model predicts gaps in MgB₂ whose ratio and temperature dependence agree fairly well with detailed calculations employing the Eliashberg theory of superconductivity² [cf. Fig. 1(a)]. We therefore use the model of Eq. (1) to calculate absorption spectra in MgB₂ in the hope that the results will apply at least qualitatively.

To calculate the absorption coefficients, we use the canonical transformation approach as described, for example, in Tinkham.¹⁸ If there are multiple gaps, one may generalize the standard single-gap expression for the coherence factors $(uv' \pm vu')^2$ and $(uu' \mp vv')^2$ by replacing Δ^2 in these expressions by $\Delta\Delta'$ (in the notation of Ref. 18), so that, e.g.,

$$(uu' \mp vv')^2 = \frac{1}{2} \left(1 + \frac{\xi\xi'}{EE'} \mp \frac{\Delta\Delta'}{EE'} \right). \quad (2)$$

Here the upper and lower signs correspond to the so-called case I and case II coherence factors determined by the time-

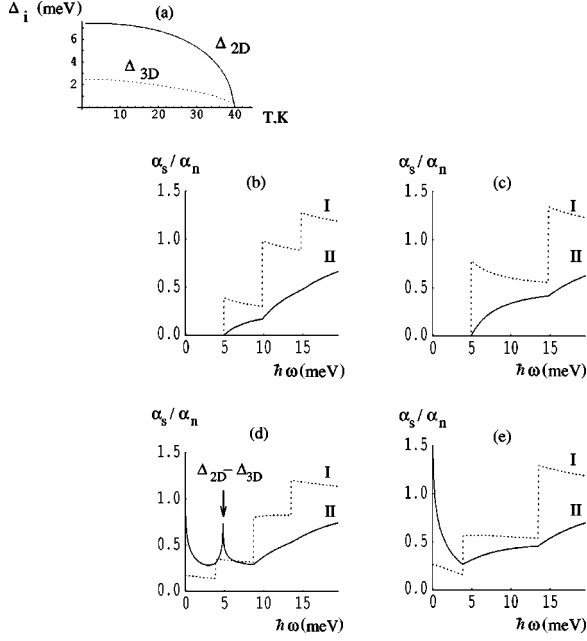


FIG. 1. (a) The temperature dependence of the two gaps for the model discussed in the text. (b) and (c) The frequency dependence of the case I and case II absorption coefficients for the same model (normalized to the normal state values) at $T=0.05T_c$ assuming (b) Eq. (9) and (c) Eq. (10) for the transition matrix elements. (d) and (e) Same as (b) and (c) but with $T=0.5T_c$.

reversal symmetry of the matrix elements. If the $N_j(\xi)$'s near the Fermi level are constant for each band and equal to $N_j(0)$, and if the electron-phonon interaction is linear (both in ξ and in the ionic displacements u), so that the upper and lower limits of integration in Eq. (1) are equal, then the terms linear in ξ and ξ' cancel when the integral over the coherence factors is carried out. Both of these assumptions may fail to some extent in MgB_2 [in particular, the electron-phonon interaction in MgB_2 is exceptionally nonlinear in u (Refs. 1 and 19)]. We will nevertheless assume that the cancellation is almost complete and neglect the terms linear in ξ and ξ' in Eq. (2).²⁰ We also assume that the matrix elements M_{ij} for a one-electron transition between an electronic state in band i and a state in band j are the same for all states in given bands i and j . The transition rate in the superconducting state induced by a perturbation of frequency ω is then found to be proportional to

$$\alpha_S = \sum_{ij} |M_{ij}|^2 N_i(0) N_j(0) I_{ij}, \quad (3)$$

$$I_{ij} \equiv \int \frac{|E(E + \hbar\omega) \mp \Delta_i \Delta_j|}{\sqrt{E^2 - \Delta_i^2} \sqrt{(E + \hbar\omega)^2 - \Delta_j^2}} \times [f(E) - f(E + \hbar\omega)] dE. \quad (4)$$

Here $f(E) = 1/[e^{E/k_B T} + 1]$ is the Fermi function, and the integration in Eq. (4) extends from $-\infty$ to $+\infty$, except for the regions where the argument of either square root becomes negative. The absorption coefficient in the normal state, α_N , is given by the same formula but with all $\Delta_i = 0$.

In the single-gap case, the ratio α_S/α_N calculated from Eqs. (3) and (4) is usually referred to as the Mattis-Bardeen formula. The corresponding ratio for the multiple-gap case is readily calculated using Eqs. (3) and (4). The normal-state value is just $\alpha_N = \sum_{ij} |M_{ij}|^2 N_i(0) N_j(0) \hbar\omega$, and hence

$$\frac{\alpha_S}{\alpha_N} = \frac{\sum_{i=1}^n \sum_{j=1}^n |M_{ij}|^2 N_i(0) N_j(0) I_{ij}}{\sum_{i=1}^n \sum_{j=1}^n |M_{ij}|^2 N_i(0) N_j(0) \hbar\omega}, \quad (5)$$

with I_{ij} given by Eq. (4).

The required integrals take very simple forms at $T=0$. In this case, $f(E) = 1$ for $E < 0$ and $f(E) = 0$ otherwise, and Eq. (4) becomes

$$I_{ij}^{T=0} = \int_{\Delta_j - \hbar\omega}^{-\Delta_i} \frac{|E(E + \hbar\omega) \mp \Delta_i \Delta_j| dE}{\sqrt{E^2 - \Delta_i^2} \sqrt{(E + \hbar\omega)^2 - \Delta_j^2}}. \quad (6)$$

Introducing $k_{ij}^{(+)} \equiv (\hbar\omega)^2 - (\Delta_i + \Delta_j)^2$ and $k_{ij}^{(-)} \equiv (\hbar\omega)^2 - (\Delta_i - \Delta_j)^2$, we can write this integral in terms of complete elliptic integrals E and K . For the case I coherence factors, Eq. (6) simply reduces to

$$I_{ij}^{I,T=0} = \theta(k_{ij}^{(+)}) \sqrt{k_{ij}^{(-)}} E\left(\frac{k_{ij}^{(+)}}{k_{ij}^{(-)}}\right), \quad (7)$$

whereas for the case II factors

$$I_{ij}^{II,T=0} = \theta(k_{ij}^{(+)}) \left[\sqrt{k_{ij}^{(-)}} E\left(\frac{k_{ij}^{(+)}}{k_{ij}^{(-)}}\right) - \frac{4\Delta_i \Delta_j}{\sqrt{k_{ij}^{(-)}}} K\left(\frac{k_{ij}^{(+)}}{k_{ij}^{(-)}}\right) \right] \quad (8)$$

[the step function $\theta(x)$ appears because the upper integration limit in Eq. (6) should always be larger than the lower one].

In order to demonstrate the qualitative features of this model, we have carried out the numerical integration for the two-gap model of MgB_2 .^{1,17} Even using this model, the matrix elements M_{ij} still remain to be calculated. Now, in MgB_2 , these two gaps are thought to come from two disconnected Fermi surfaces. Since these are disjoint, the normal-state resistivity is likely to be determined primarily by *intra-band* scattering. If so, the *off-diagonal* matrix elements M_{ij} would be very small. Various scattering processes (e.g., impurity scattering, electron-phonon scattering involving a large-wave-vector phonon) could, however, produce non-zero off-diagonal matrix elements in principle. We have therefore carried out two model calculations, based on Eq. (5). In the first, we have simply made the crude assumption that all the factors $M_{ij} N_i(0) N_j(0)$ are equal, so that the Eq. (5) becomes simply

$$(\alpha_S/\alpha_N) = \left(\sum_{ij} I_{ij}/n^2 \hbar\omega \right), \quad (9)$$

where n is the number of bands. In the second, we have taken $M_{ij} = 0$ for $i \neq j$, as suggested by the above argument, but still assuming all diagonal elements $M_{ii} N_i(0)^2$ to be equal, so that

$$(\alpha_S/\alpha_N) = \left(\sum_i I_{ii}/n\hbar\omega \right). \quad (10)$$

In Figs. 1(b)–1(e), we show the transition rates as calculated from these expressions, for processes with case I (dashed lines) and case II (solid lines) coherence factors, and making either of assumption (9) or (10) at $T=0.05T_c$ and $T=0.5T_c$, as indicated. The case II coherence factors correspond to ordinary far-infrared absorption or, equivalently, the real part of the frequency-dependent conductivity. We consider two temperatures $T \sim 2$ and 20 K. At very low temperatures, the absorption spectra for assumption (9) resemble a sum of three single-gap spectra which become nonzero at the three different possible values of $\Delta_i + \Delta_j$. If the matrix elements are diagonal, the spectra would resemble the sum of *two* single-gap spectra. In either case, the lowest frequency where absorption occurs is determined by the smallest gap, which we denote Δ_{i_0} , and occurs at frequency $\omega = 2\Delta_{i_0}/\hbar$. Other absorption edges, where α_S/α_N has a slope discontinuity at $T=0$, occur at other values of $\Delta_i + \Delta_j$, but are not very prominent, especially for the case II spectra. For the present model, the smaller gap $\Delta_{3D} \approx 2.5$ meV, and the corresponding absorption edge is at $2\Delta_{3D}/k_B T_c \approx 1.4$, well below the BCS value.

The case II absorption coefficients at finite temperatures [Figs. 1(c) and 1(d)] show features not present in the lowest-temperature plots, whether the transition matrix elements are assumed to obey Eq. (9) or (10). First, there is a weak below-gap absorption for all frequencies $\hbar\omega < 2\Delta_{i_0}$. This absorption is also present in the single-gap case. But in the multiple-gap superconductor, this background absorption, together with the peak feature discussed below, may mask the case II absorption edge at $2\Delta_{i_0}$. (This edge is still visible for case I spectra, even at finite T .) Instead, for case II spectra, one of the secondary edges at $\Delta_i + \Delta_j > 2\Delta_{i_0}$ may become more prominent than the minimum absorption edge. In addition, if the *nondiagonal* matrix elements are substantial as in Eq. (9), there is an extra peak at the frequency of the *gap difference*, $\hbar\omega_{ij} = |\Delta_i - \Delta_j|$. At this frequency, the integrand in Eq. (4) has two multiplicative singularities [square roots in the denominator of Eq. (4)] As a result, the α_S calculated from Eqs. (3) and (4) is proportional to $-\ln(|\omega - \omega_{ij}|)$, with a coefficient which is proportional to the number of thermally excited quasiparticles. However, if the matrix elements satisfy the diagonality assumption (10), this extra peak is absent. The origin of this peak(s) is the same as that of the better-known peak at $\omega = 0$ in the single-gap case. This latter peak is responsible for the rise of the nuclear relaxation rate $1/T_1$ to a value exceeding the normal-state value as the superconductor is cooled through T_c .²¹ As in the $1/T_1$ case, the actual height and width of the peak at $|\Delta_i - \Delta_j|$ can be determined only when the \mathbf{k} dependence of the superconducting gaps, $\Delta_i(\mathbf{k})$, is included.

We now move on to discuss recent measurements of the infrared conductivity in MgB₂ films.¹⁴ In Fig. 2 (adapted from Fig. 2 of Ref. 14), we show the measured real part of the optical conductivity, $\sigma_1(\omega)$, normalized to its value in

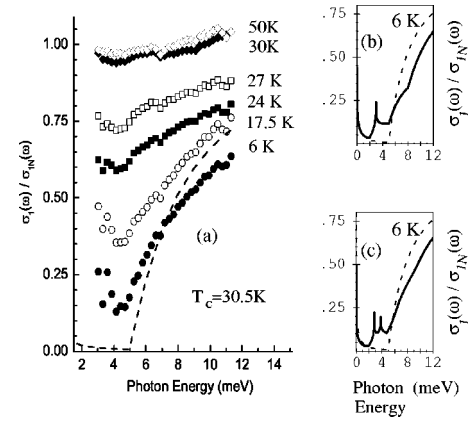


FIG. 2. (a) Symbols: experimental $\sigma_1(\omega)$, scaled to the 40 K value in the normal state, as measured on a 100-nm-thick film of MgB₂ ($T_c \approx 30.5$ K) (adapted from Ref. 13). The dashed line shows the fit of the 6 K data to the single-gap Mattis-Bardeen expression (with $2\Delta = 5$ meV), as given in Ref. 13. (b),(c) Calculated $\sigma_1(\omega)/\sigma_N(\omega)$ for (b) a two-gap or (c) a three-gap model, assuming nonzero off-diagonal transition matrix elements as discussed in the text (solid lines), and for a BCS single-gap model (dashed lines) using $2\Delta = 5$ meV.

the normal state at 40 K, $\sigma_{1N}(\omega)$. These data show several unusual features. First, there is an apparent absorption edge at 5 meV (well below both the weak- and strong-coupling single-gap BCS values) and a large background absorption below this edge. Second, the experimental data show a weaker and more slowly rising σ_{1S}/σ_{1N} ratio above the apparent absorption edge than a single-gap Mattis-Bardeen calculation (shown for $2\Delta = 5$ meV and $T = 6$ K as a dashed line). Finally, these spectra appear to have a characteristic structure between 3 and 4 meV, present only in the superconducting state and reminiscent of the peak structure discussed above. However, this experimentally observed structure could lie within the experimental uncertainty, which is largest at low frequencies, where it is comparable to the scatter in the data points.²² Indeed, earlier data by Pronin *et al.*²³ is inconclusive regarding the presence of such 3–4 meV structure. More accurate measurements are needed to determine whether the peak structure is actually present in the MgB₂ spectra.

Clearly, the simple model of in Fig. 1 cannot be directly applied to the measurements shown in Fig. 2. First, the ω_D parameter of the BCS model (1) was chosen to give $T_c \sim 40$ K, whereas the sample of Fig. 2 has $T_c \sim 30.5$ K. At minimum, we should multiply all the energy and temperature parameters used to obtain Fig. 1 by a factor of $\sim 3/4$, to account for this lower T_c . Also, the factors $M_{ij}N_i(0)N_j(0)$ need not be independent of i and j , as was assumed for Figs. 1(b) and 1(c), and the factors $M_{ii}N_i(0)^2$ need not be independent of i as assumed in Fig. 1(d); these factors could also depend on the polarization of the radiation. Finally, the actual distribution of gap values should be included. In the clean limit this distribution $[\Delta_i(\mathbf{k})]$ is predicted to be broad and to have several peaks in both “2D” and “3D” regions.² But impurity scattering should lead to “averaging” of the gap values in the experimental sample ($l \sim 100$ Å). The re-

sulting gap distribution depends strongly on the relative magnitudes of various scattering rates, and in MgB_2 these rates are thought to be small for scattering *between* 2D and 3D states,^{13,24} thus justifying the use of a “two-gap” model, as mentioned above. But for relatively small impurity concentrations, the gap values should still have some dispersion around the average Δ_{2D} and Δ_{3D} . The clean-limit results of Ref. 2 suggest that two slightly different gaps $\Delta_{2D,1}$ and $\Delta_{2D,2}$ might form on the two 2D Fermi surfaces if the *intra-band* scattering is stronger than scattering between two different 2D bands, for relatively clean samples.

To illustrate these effects, we have calculated α_S/α_N for case II coherence factors using Eqs. (4) and (5), with parameters *arbitrarily* chosen so as to give a reasonable fit between the calculated results and the measured α_S/α_N . To illustrate possible effects of nontrivial gap value distribution, we used either two gaps (Δ_{2D} and Δ_{3D}) or three gaps ($\Delta_{2D,1}$, $\Delta_{2D,2}$, and Δ_{3D}). In both cases, we have assumed that the off-diagonal matrix elements are substantial.²⁵ The calculated curves shown in the insets of Fig. 2 (solid line) have most of the features of experiment: an apparent absorption edge at a frequency well below the single-gap BCS value, a large background absorption below this edge²⁶ at finite T , and a more slowly rising $\alpha_S(\omega)/\alpha_N(\omega)$ with increasing frequency above the absorption edge than is predicted by the single-gap BCS model (inset of Fig. 2, dashed line). However, we em-

phasize that the extra sharp peaks in the insets are present only if the off-diagonal matrix elements M_{ij} are substantial, which may well not be the case in MgB_2 .

In conclusion, we have presented a simple calculation of far-infrared absorption in a model for MgB_2 , using a generalization of the Mattis-Bardeen formula to several gaps. The resulting absorption ratio $\alpha_S(\omega)/\alpha_N(\omega)$ shows a qualitative resemblance to the measured results. Specifically, the onset of absorption at a frequency well below the onset predicted by isotropic BCS theory, large background absorption below the apparent absorption edge, and a slower rise of $\alpha_S(\omega)/\alpha_N(\omega)$ than in the single-gap case are all easily reproduced by the multiple-gap model. Thus, the recent optical conductivity measurements¹⁴ appear to be consistent with the hypothesis of multiple superconducting gaps in MgB_2 . If certain interband transition matrix elements are sufficiently large, the multiband model would lead to a peak at a frequency corresponding to the gap difference $\Delta_{2D} - \Delta_{3D}$, which might be observable at finite temperatures in moderately dirty samples.

This work has been supported by NSF through Grant No. DMR 01-04987 and the U.S.-Israel Binational Science Foundation, and also benefited from the computational facilities of the Ohio Supercomputer Center. We thank T. R. Lemberger for valuable conversations.

- ¹A. Y. Liu, I. I. Mazin, and J. Kortus Phys. Rev. Lett. **87**, 087005 (2001).
²H. J. Choi *et al.*, Phys. Rev. B **66**, 020513 (2002); cond-mat/0111183 (unpublished).
³Both $\Delta_{2D}(\mathbf{k})$ and $\Delta_{3D}(\mathbf{k})$ are calculated to be essentially isotropic (i.e., only weakly dependent on \mathbf{k}); the subscripts here refer to the topologies of the corresponding Fermi surfaces.
⁴F. Bouquet *et al.*, Phys. Rev. Lett. **87**, 047001 (2001); R. A. Fisher *et al.*, in *Studies of High Temperature Superconductors*, Vol. 38, edited by A. V. Narlikar (Nova Science, Commack, NY, 2001); F. Bouquet *et al.*, Europhys. Lett. **56**, 856 (2001).
⁵A. A. Golubov *et al.*, J. Phys.: Condens. Matter **14**, 1353 (2002).
⁶H. Schmidt *et al.*, Phys. Rev. Lett. **88**, 127002 (2002).
⁷Yu. G. Naidyuk *et al.*, JETP Lett. **75**, 238 (2002).
⁸A. Brinkman *et al.*, Phys. Rev. B **65**, 180517 (2002).
⁹A. I. D'yachenko *et al.*, cond-mat/0201200 (unpublished).
¹⁰S. Tsuda *et al.*, Phys. Rev. Lett. **87**, 177006 (2001).
¹¹M.-S. Kim *et al.*, cond-mat/0201550 (unpublished).
¹²D. C. Mattis and J. Bardeen, Phys. Rev. **111**, 412 (1958).
¹³I. I. Mazin *et al.*, Phys. Rev. Lett. **89**, 107002 (2002).
¹⁴R. A. Kaindl *et al.*, Phys. Rev. Lett. **88**, 027003 (2002).
¹⁵S. B. Nam, Phys. Rev. **156**, 470 (1967); **156**, 487 (1967); P. B. Allen, Phys. Rev. B **3**, 305 (1971).
¹⁶O. Klein *et al.*, Phys. Rev. B **50**, 6307 (1994).
¹⁷From the parameters of Ref. 1 the products $\Lambda_{ij} \equiv U_{ij}N_j(0)$ take the values $\Lambda_{11}=0.96$, $\Lambda_{12}=0.16$, $\Lambda_{21}=0.22$, and $\Lambda_{22}=0.28$, with “1” referring to the 2D and “2” to the 3D bands. The

- values of T , Δ_i , and ω are then all scaled by a single BCS cutoff parameter ω_D . $T_c \approx 40$ K corresponds to $\omega_D \approx 7.5$ meV.
¹⁸M. Tinkham, *Introduction to Superconductivity*, 2nd ed. (McGraw-Hill, New York, 1996), pp. 79–89.
¹⁹T. Yildirim *et al.*, Phys. Rev. Lett. **87**, 037001 (2001).
²⁰To calculate corrections resulting from any noncancellation of linear terms in Eq. (2) would require a treatment more elaborate than the BCS picture discussed here.
²¹Y. Masuda, Phys. Rev. **126**, 1271 (1962).
²²R. A. Kaindl (private communication).
²³A. V. Pronin *et al.*, Phys. Rev. Lett. **87**, 097003 (2001).
²⁴A. A. Golubov and I. I. Mazin, Phys. Rev. B **55**, 15 146 (1997).
²⁵For the calculations in the insets of Fig. 2 we used the following parameters: For inset (b), $\Delta_{2D}=4$ eV, $\Delta_{3D}=1$ eV; for the matrix elements (in units such that $|M_{2D,2D}|^2=1$): $|M_{2D,3D}|^2=.25$, $|M_{3D,3D}|^2=0.125$. For inset (c), $\Delta_A=3.8$, $\Delta_B=4.8$, $\Delta_C=1$. (We use the compressed notation $A \equiv 2D, 1$; $B \equiv 2D, 2$; $C \equiv 3D$.) For the matrix elements (in units such that $|M_{AA}|^2=1$): $|M_{AB}|^2=2$, $|M_{AC}|^2=1$, $|M_{BB}|^2=10$, $|M_{BC}|^2=2$, $|M_{CC}|^2=0.3$. The values of $N_A(0)$, $N_B(0)$ and $N_C(0)$ were taken from Ref. 1 [1.38, 0.66, and 2.78 states/(Ry spin primitive cell)].
²⁶The apparent absorption edge at ~ 5 meV in our fitted model is actually due to transitions between the 2D and 3D bands that begin at $\Delta_{2D} + \Delta_{3D}$ (or $\Delta_{2D,1} + \Delta_{3D}$). The true $T=0$ absorption edge is at $2\Delta_{3D}=2$ meV and is responsible for the large background below 5 meV, again consistent with experiment.